First Demonstration of Compact, Ultra-Thin Low-Pass and Bandpass Filters for 5G Small-Cell Applications

Muhammad Ali, Fuhan Liu, Atom Watanabe, P. Markondeya Raj, Venkatesh Sundaram, Manos M. Tentzeris, and Rao R. Tummala

***Abstract*— Package-integrated and ultra-thin low-pass filter (LPF) and bandpass filter (BPF) with footprint smaller than $0.5\lambda_0 \times 0.5\lambda_0 \times 0.025\lambda_0$ at the operating frequencies of 28- and 39-GHz bands are presented for 5G and mm-wave small-cell application. Such package integration of 5G filters with ultrashort 3-D interconnects allows for low interconnect losses that are similar to that of on-chip filters, but low component insertion loss of off-chip discrete filters. These thin-film filters exhibit a cross-sectional height of 188.5 μm and can be utilized either as embedded components or integrated passive devices in module packages. Three topologies of LPF and BPF in total are modeled, designed, and fabricated on precision thin-film buildup layers on glass substrate as a core. Large-area panel-compatible semiadditive patterning (SAP) process is utilized to form high-precision topologies to aid the low-cost fabrication of ultraminiaturized filters. SAP also enables the realization of ultra-thin traces to precisely model high-impedance inductive lines compared to conventional subtractive etching and printing techniques. This results in filters with low insertion loss, low VSWR, and high selectivity. The simulated and measured results of filters show an excellent correlation.**

***Index Terms*— 5G and mm-wave, filter, hairpin, interdigital, quasi-lumped, RF, semiadditive process, small cell.**

I. Introduction

WIRELESS communication systems are the major facilitators for the ubiquity of smartphones. Advancements in these systems are playing a prominent role in realizing the envisioned form of Internet of Things, self-driving cars with vehicle-to-vehicle and vehicle-to-everything connectivity, and combining multiple communication standards in modern devices for a range of applications. The major breakthroughs are driven by these technologies in realms of electronics and packaging for multiband multistandard communications such as long-term evolution and mm-wave standards. Miniaturized individual components and modules with increased functional density and reduced footprint are essential to meet the growing demand for mm-wave band small cells in the 5G infrastructure [1]. 5G wireless systems will use mm-wave frequency bands, 28-GHz U.S. (24.5–29.5 GHz) and 39-GHz EU (37.0–43.5 GHz), to provide fast data rates of 100 Mb/s to the end users in metropolitan areas.

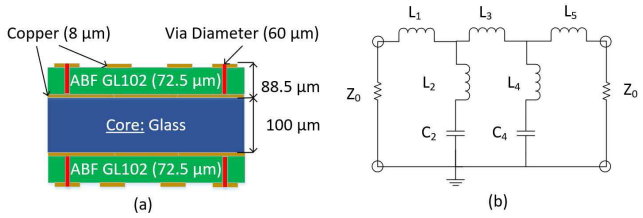

Fig. 1. (a) Material stackup for demonstration of filters. (b) *LC* prototype schematic of a fifth-order elliptical LPF with finite-frequency attenuation poles.

Traditionally, mm-wave components are designed on-chip to take advantage of tight process control. However, this can consume expensive IC real estate and also lead to high component insertion loss. Traditional package integration with thick components can lead to large interconnect loss and prevent design flexibility. Package integration with ultra-thin 3-D architectures can address the limitations of both on-chip and off-chip approaches and gives the best performance of both. Semiadditive patterning (SAP) process enables the realization of precision circuitry on ultra-thin materials such as glass and is superior to conventional processes such as wet etching in which feature profile and dimensions are difficult to control when high precision (on the order of few micrometers) is required [2]. Glass is an ideal core material for mm-wave 5G modules and integrated passive devices (IPDs) since it combines the benefits of ceramics for high-frequency electrical performance, laminates for large-area panel processing and low cost, and silicon for its dimensional stability and precision patterning, which is essential for mm-wave circuits. This empowers the realization of compact, low loss, and high-selectivity filters which can be either embedded as thin films into the package or prefabricated as standalone IPDs that can be embedded in a 3-D module [3].

Manuscript received September 23, 2018; accepted October 9, 2018. Date of publication November 5, 2018; date of current version December 4, 2018. *(Corresponding author: Muhammad Ali).*

M. Ali, F. Liu, A. Watanabe, V. Sundaram, M. M. Tentzeris, and R. R. Tummala are with the School of Electrical and Computer Engineering, Georgia Institute of Technology, Atlanta, GA 30332 USA (e-mail: ali_cmi@gatech.edu).

P. M. Raj is with the School of Electrical and Computer Engineering, Georgia Institute of Technology, Atlanta, GA 30332 USA, and also with the Department of Biomedical Engineering, Florida International University, Miami, FL 33199 USA.

Color versions of one or more of the figures in this paper are available online at http://ieeexplore.ieee.org.

Digital Object Identifier 10.1109/LMWC.2018.2876769

II. Filter Design and Fabrication

A. Material Stackup

The material stackup for this demonstration is shown in Fig. 1(a). A 72.5-μm-thick epoxy film from Ajinomoto (ABF GL102), laminated onto a 100-μm glass core, is chosen as the substrate for the filters. The film depicts a Dk of 3.3 and a Df of 0.0044 at 5.8 GHz and has stable electrical properties up to 50 GHz. The design rules are also set at this stage of the modeling process and are listed as follows.

1) *Critical Dimension (Minimum Width) and Linespace:* >15 μm.
2) *Copper Thickness:* 8 μm.
3) *Via Diameter:* 60 μm.

B. Filter Design

Two types of filters, low-pass filter (LPF) and bandpass filter (BPF), are chosen for this letter. Quasi-lumped elliptical LPFs are selected for their sharpest rolloff. The BPFs are further subdivided into two structures: interdigital and hairpin. These filters are based on $\lambda/4$ short and $\lambda/2$ open resonators, respectively, making them ideal for small footprint. The design process of elliptical LPFs starts with a low-pass prototype with an elliptical response. The prototype is shown in Fig. 1(b) and the design methodology is summarized in the following.

1) Select g-values for the desired order, then scale them to the desired impedance and operating frequency to find LC values using the following equation:

$$L_i = \frac{1}{2\pi f_c} Z_0 g_{Li} \quad C_i = \frac{1}{2\pi f_c} \frac{1}{Z_0} g_{Ci} \tag{1}$$

where f_c is the cutoff frequency of LPF, Z_0 is the characteristic impedance (usually 50 Ω), and g_{Li} and g_{Ci} are the g-values of the filter corresponding to inductors and capacitors.

2) The following equation can be used to find the physical length corresponding to each lumped LC for microstrip structure:

$$l_{Li} = \frac{\lambda_{gL}(f_c)}{2\pi} \arcsin\left(2\pi f_c \frac{L_i}{Z_{0L}}\right)$$
$$l_{Ci} = \frac{\lambda_{gC}(f_c)}{2\pi} \arcsin(2\pi f_c Z_{0C} C_i) \tag{2}$$

where $\lambda_{gL}(f_c)$ and $\lambda_{gC}(f_c)$ are the guide wavelengths, and $Z_{0L}(> Z_0)$ and $Z_{0C}(< Z_0)$ are the characteristic impedances of inductor and capacitor transformations (set by the designer).

The design rules enable the highest impedance to be 127 Ω (15 μm), which aids in modeling inductors in LPFs more effectively. However, the minimum width during Keysight ADS simulations is restricted to 20 μm (119 Ω) to mitigate the effects of process variations on filter performance. BPF filter design methodology is given in detail in [4] and [5]. Several LPFs and BPFs of different orders are synthesized for this demonstration.

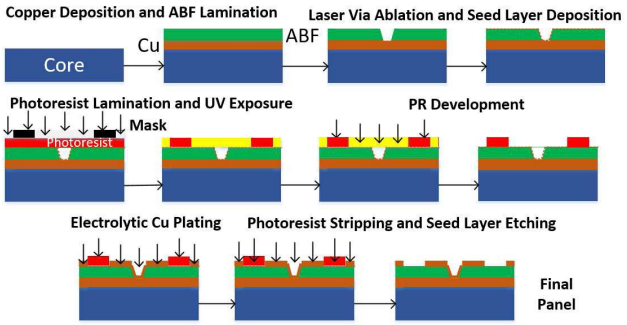

Fig. 2. Schematic step-by-step illustration of SAP with cross sections.

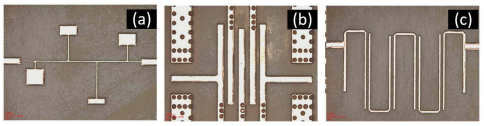

Fig. 3. Fabricated filters for 28-GHz band. (a) Ninth-order LPF. (b) Fifth-order interdigital BPF. (c) Fifth-order hairpin BPF.

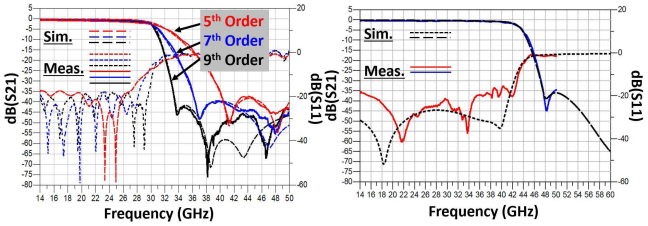

Fig. 4. Simulated and measured results of fabricated LPFs. (a) Fifth, seventh, and ninth orders for 28-GHz band. (b) Ninth order for 39-GHz band.

C. Fabrication Process

The fabrication process utilizes the SAP process to pattern the copper structures. Fig. 2 illustrates the SAP process through schematic cross sections of each step. The process starts with a bare glass panel on which copper is electrolytically deposited. Next, the dielectric film is laminated, vias are drilled in it, and a copper seed layer is deposited. The panel is photolithographically patterned, followed by photoresist development and electrolytic plating. Critical process steps are exposure (dose) time, via ablation conditions, photoresist development speed, and electrolytic plating. Finally, the photoresist is removed and the seed layer is etched away to obtain the desired circuit. After the fabrication process, the measured copper thickness is 8.5 ± 0.5 μm. Three of the fabricated filters are shown in Fig. 3.

III. Characterization Results and Analysis

This section discusses the characterization results of the fabricated filters. The measurements are performed using a Keysight E8361C PNA in the frequency range of 14–50 GHz using ACP50 GSG probes and short-open-load-through calibration. The comparison of the simulated and measured results of LPFs for 28 and 39 GHz band is shown in Fig. 4. Similarly, the results of the fabricated third- and fifth-order interdigital and hairpin BPFs for 28- and 39-GHz band are shown in Figs. 5 and 6, respectively. The filters exhibit

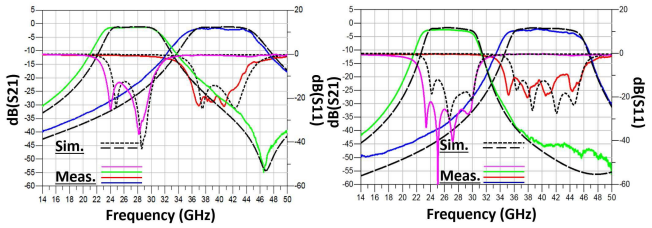

(a) (b)

Fig. 5. Simulated and measured results of interdigital BPFs for 28 and 39-GHz band. (a) Third order. (b) Fifth order.

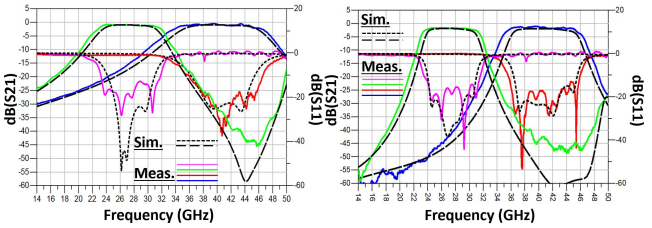

(a) (b)

Fig. 6. Simulated and measured results of hairpin BPFs for 28 and 39-GHz band. (a) Third order. (b) Fifth order.

TABLE I

PHYSICAL AND ELECTRICAL DIMENSIONS OF FABRICATED HIGHER ORDER FILTERS

Filter	Physical Dimensions (mm^3)	Electrical Dimensions $(\lambda_0)^3$
9^{th} order LPF for 28 GHz band	4.59×1.70×0.1885	0.43×0.16×0.018
5^{th} order Interdigital BPF for 28 GHz band	3.06×2.25×0.1885	0.29×0.21×0.018
5^{th} order Interdigital BPF for 39 GHz band	3.12×1.77×0.1885	0.41×0.23×0.025
5^{th} order Hairpin BPF for 28 GHz band	4.65×2.12×0.1885	0.43×0.19×0.018
5^{th} order Hairpin BPF for 39 GHz band	3.85×1.66×0.1885	0.50×0.22×0.025

excellent model-to-hardware correlation with low insertion loss, high selectivity (30-dB attenuation point to band-edge ratio of 1.24 maximum), and a large positive return loss (low VSWR), indicating a good impedance match.

The physical and electrical dimensions of the highest order filters are given in Table I. The physical dimensions are normalized with free-space wavelengths corresponding to 28 and 39 GHz, which are 10.71 and 7.69 mm, respectively. As evident from Table I, the footprint of the fabricated filters is smaller than $0.5\lambda_0 \times 0.5\lambda_0 \times 0.025\lambda_0$, with a height of 188.5 μm. A performance comparison between this letter and other similar filter structures in the literature is presented in Table II. A thorough search of the relevant literature yielded that the demonstrated filters are smallest in terms of xy dimensions as well as z height. Moreover, they depict superior performance in terms of in-band insertion loss and out-of-band rejection.

IV. CONCLUSION

Miniaturized high-performance filters with footprint less than half the free-space wavelength at the operating frequency

TABLE II

COMPARISON WITH SIMILAR FILTERS

Ref. Filter	Type	f_0 (GHz) & FBW (%)	Insertion Loss	Size $(\lambda_0)^3$
[6] - 4^{th} order	Vertically Stacked SIW on LTCC	29.87 & 13%	3.3 dB	0.37×0.28×0.08
[7] - 4^{th} order	Stacked SIW on LTCC	27.95 & 3.7%	2.8 dB	0.57×0.30×0.04
[8] - 3^{rd} order	SIW Resonator on PCB	35.8 & 13%	3 dB	0.94×0.51×0.03
[9] - 4^{th} order	Edge-Coupled Microstrip on PCB	38.5 & 0.08%	3 dB	0.60×0.31×0.03
This work - 5^{th} order	Interdigital BPF on Glass	27.0 & 18.52%	2.6 dB	0.29×0.21×0.018
This work - 5^{th} order	Hairpin BPF on Glass	40.25 & 16.15%	1.43 dB	0.50×0.22×0.025

of 28- and 39-GHz bands are demonstrated on thin substrates for 5G small-cell applications. Two filter types, with three topologies in total are modeled, designed, optimized, fabricated, and characterized. The filters are fabricated using an optimized SAP process to meet the dimensional accuracy required by these filtering structures. The characterization results showed excellent correlation with the simulated response from all the fabricated filters. Integration in ultra-thin 3-D glass packages with ultrashort interconnections results in on-chip-like interconnect losses but with superior performance. The fabricated filters depict low insertion loss, high out-of-band rejection, and low VSWR. Small footprint of the filters, combined with their reduced height, makes them ideal for several 5G and mm-wave applications.

REFERENCES

[1] P. Mogensen *et al.*, "5G small cell optimized radio design," in *Proc. IEEE Globecom Workshops (GC Wkshps)*, 2013, pp. 111–116.

[2] P. M. Raj *et al.*, "'zero-undercut' semi-additive copper patterning—A breakthrough for ultrafine-line rdl lithographic structures and precision RF thinfilm passives," in *Proc. IEEE 65th Electron. Compon. Technol. Conf. (ECTC)*, May 2015, pp. 402–405.

[3] M. Ali *et al.*, "Miniaturized high-performance filters for 5G small-cell applications," in *Proc. IEEE 68th Electron. Compon. Technol. Conf. (ECTC)*, May 2018, pp. 1068–1075.

[4] J.-S. G. Hong and M. J. Lancaster, *Microstrip Filters for RF/Microwave Applications*, vol. 167. Hoboken, NJ, USA: Wiley, 2004.

[5] G. L. Matthaei, L. Young, and E. M. T. Jones, *Microwave Filters, Impedance-Matching Networks, and Coupling Structures*. New York, NY, USA: McGraw-Hill, 1964.

[6] T. M. Shen, T. Y. Lin, T. Y. Huang, and R. B. Wu, "A vertically stacked quasi-elliptic waveguide filter with crossly coupling vias," in *Proc. Asia–Pacific Microw. Conf.*, Dec. 2007, pp. 1–4.

[7] K. S. Chin, C. C. Chang, C. H. Chen, Z. Guo, D. Wang, and W. Che, "LTCC multilayered substrate-integrated waveguide filter with enhanced frequency selectivity for system-in-package applications," *IEEE Trans., Compon., Packag., Manuf., Technol.*, vol. 4, no. 4, pp. 664–672, Apr. 2014.

[8] Y. Tao, W. Hong, and H. Tang, "Design of a Ka-band bandpass filter based on high order mode siw resonator," in *Proc. 7th Int. Symp. Antennas, Propag. EM Theory*, Oct. 2006, pp. 1–3.

[9] Y. M. Yan, Y. T. Chang, H. Wang, R. B. Wu, and C. H. Chen, "Highly selective microstrip bandpass filters in Ka-band," in *Proc. 32nd Eur. Microw. Conf.*, Sep. 2002, pp. 1–4.